(Alkylperoxo)platinum(IV) Complexes Formed by Oxidative Addition of Alkyl Halides in the Presence of Oxygen: The Mechanism of Reaction and the Structure of *trans*-Iodo(isopropylperoxo)dimethyl(1,10-phenanthroline)-platinum(IV)

George Ferguson,*[1a] Patrick K. Monaghan,[1b] Masood Parvez,[1a] and Richard J. Puddephatt*[1b]

Departments of Chemistry, The University of Guelph, Guelph, Ontario, Canada N1G 2W1, and University of Western Ontario, London, Ontario, Canada N6A 5B7

Received February 5, 1985

Reaction of $[PtMe_2(NN)]$ (1, NN = 1,10-phenanthroline or 2,2′-bipyridyl) with *i*-PrX under inert atmosphere gives $[PtXMe_2$-*i*-Pr$(NN)]$ (2, X = Br; 3, X = I) but, in the presence of oxygen, *i*-PrI reacts to give a mixture of 3, $[PtIMe_2(OO$-*i*-Pr$)(NN)]$, 4, and $[PtI_2Me_2(NN)]$, 5. The reaction with *i*-PrBr occurs by the S_N2 mechanism, but with *i*-PrI the mechanism is largely free radical in nature. Oxygen acts as a reagent to trap the intermediate *i*-Pr· radicals, is incorporated into the product 4, and acts as an inhibitor of the free radical chain reaction. The reactions with *i*-PrI are greatly accelerated by light; in the dark and in the presence of free radical inhibitors such as oxygen, the S_N2 mechanism is thought to operate to a minor extent. *t*-BuI reacts with $[PtMe_2(NN)]$ in the presence of air to give $[PtIMe_2(OO$-*t*-Bu$)(NN)]$. These are the first (alkylperoxo)platinum(IV) complexes. The structure of $[PtIMe_2(OO$-*i*-Pr$)(NN)]$ was determined by X-ray crystallography. Crystals are monoclinic, space group $P2_1/n$, with four molecules in a cell of dimensions a = 9.946 (2) Å, b = 11.340 (3) Å, c = 16.374 (2) Å, and β = 94.55 (1)°. The structure was solved by the heavy-atom method and refined by full-matrix least-squares calculations with anisotropic thermal parameters for the non-hydrogen atoms. At convergence, R = 0.0230 and R_w = 0.0242 for 1402 observed data. The Pt atom has octahedral coordination, with trans oxygen and iodine atoms. Principal dimensions are Pt–O(1) = 2.032 (6) Å, Pt–I = 2.624 (1) Å, Pt–Me = 2.048 and 2.067 (8) Å, Pt–N = 2.164 and 2.175 (7) Å, O(1)–O(2) = 1.465 (9) Å, and Pt–O(1)–O(2) = 110.2 (4)°.

Introduction

There has been considerable interest in the mechanisms of oxidative addition of alkyl halides to transition-metal complexes.[2,3] Three mechanisms have been established (eq 1–3). The first involves S_N2 displacement of the halide

$$L_nM + RX \rightarrow [L_nMR]^+X^- \rightarrow L_nMXR \quad (1)$$

$$L_nM + R\cdot \xrightarrow{RX} [L_nMR]\cdot \xrightarrow{RX} L_nMXR + R\cdot \quad (2)$$

$$L_nM + RX \rightarrow [L_nM]^+\cdot[RX]^-\cdot \rightarrow [L_nMX]\cdot + R\cdot \rightarrow L_nMXR \quad (3)$$

by a metal nucleophile, the second involves a free radical chain reaction, and the third involves a free radical non-chain mechanism, perhaps initiated by electron transfer to the alkyl halide.[2-5]

It is now clear that the mechanism adopted depends on the metal substrate, the alkyl halide, and the reaction conditions.[2-5] Furthermore, the tests used to distinguish between mechanisms 1–3 are often equivocal, and a combination of tests is usually required.[2-5]

In earlier papers the oxidative addition reactions of methyl iodide and primary alkyl iodides with $[PtMe_2(NN)]$ (**1a**, NN = 1,10-phenanthroline; **1b**, NN = 2,2′-bipyridyl) have been shown to occur by the S_N2 mechanism of eq 1.[6,7] Now the reactions of complexes **1a** and **1b** with the secondary and tertiary alkyl halides *i*-PrBr, *i*-PrI, and *t*-BuI have been studied. During these studies, the first (alkylperoxo)platinum(IV) complexes have been prepared and characterized. Very few stable alkylperoxo derivatives of transition metals are known[8-12] though they have been implicated as reaction intermediates in such metal-catalyzed reactions as the autoxidation of alkanes and alkenes and the epoxidation of alkenes with alkyl hydroperoxides, as well as in the autoxidation of many transition-metal alkyl derivatives.[13-16] The formation of these alkylperoxo derivatives also gives a useful test for a free radical mechanism of oxidative addition. A preliminary account of parts of this work has been published.[17]

Results and Discussion

Reaction with Isopropyl Bromide. The reaction of **1a** with *i*-PrBr in acetone was extremely slow and gave only the product of trans oxidative addition **2a**, which was easily characterized by the ^1H NMR spectrum. Reaction of mixtures of *i*-PrBr and *n*-PrBr with **1a** gave mixtures of **2a** and **2b** as products, and the product ratio, as measured by integration of the MePt resonance in the ^1H NMR spectra for each, was given by **2a**/**2b** α [*i*-PrBr]/[*n*-PrBr]

(1) (a) University of Guelph. (b) Univeristy of Western Ontario.
(2) Lappert, M. F.; Lednor, P. W. *Adv. Organomet. Chem.* **1976**, *14*, 345.
(3) Kochi, J. K. "Organometallic Mechanisms and Catalysis"; Academic Press: New York, 1978; Chapter 7.
(4) Labinger, J. A.; Osborn, J. A.; Coville, N. J. *Inorg. Chem.* **1980**, *19*, 3236. Kramer, A. V.; Osborn, J. A. *J. Am. Chem. Soc.* **1974**, *96*, 7832.
(5) Hall, T. L.; Lappert, M. F.; Lednor, P. W. *J. Chem. Soc., Dalton Trans.* **1980**, 1448.
(6) Monaghan, P. K.; Puddephatt, R. J. *Inorg. Chim. Acta* **1983**, *76*, L237.
(7) Jawad, J. K.; Puddephatt, R. J. *J. Chem. Soc., Dalton Trans.* **1977**, 1466.
(8) Strukul, G.; Michelin, R. A.; Orbell, J. D.; Randaccio, L. *Inorg. Chem.* **1983**, *22*, 3706.
(9) Mimoun, H.; Charpentier, R.; Mitschler, A.; Fischer, J.; Weiss, R. *J. Am. Chem. Soc.* **1980**, *102*, 1047.
(10) Booth, B. L.; Haszeldine, R. N.; Neuss, G. R. H. *J. Chem. Soc., Dalton Trans.* **1982**, 37.
(11) Fontaine, C.; Duong, K. N. V.; Merienne, C.; Gaudemer, A.; Giannotti, C. *J. Organomet. Chem.* **1972**, *38*, 167.
(12) Chiaroni, A.; Pascard-Billy, C. *Bull. Soc. Chim. Fr.* **1973**, 781.
(13) Kochi, J. K. "Free Radicals"; Wiley: New York, 1973; Chapters 10, 12, and 13.
(14) Brindley, P. B.; Hodgson, J. C. *J. Organomet. Chem.* **1974**, *65*, 57.
(15) Kollar, J. U.S. Patent 33 504 422, 1967; U.S. Patent 3 351 635, 1967.
(16) Mimoun, H. Angew. *Chem., Int. Ed. Engl.* **1982**, *21*, 734.
(17) Ferguson, G.; Parvez, M.; Monaghan, P. K.; Puddephatt, R. J. *J. Chem. Soc., Chem. Commun.* **1983**, 267.

0276-7333/85/2304-1669$01.50/0

Table I. Product Ratios for the Reaction of Complex 1a with Isopropyl Iodide in Acetone

	concn/M			products, %		
	10^3[1a]	[*i*-PrI]	$10^3[O_2]$	3a	4a	5
(i)	3.9	0.6	0[a]	100	0	0
(ii)	4	0.5	11[b]	8	89	3
(iii)	15	0.167	2[b]	44	51	5
(iv)	7.7	0.167	2[b]	34	56	10
(v)	2.4	0.167	2[b]	0	63	37
(vi)	8.8	0.33	2[b]	17	58	25
(vii)	8.8	0.33	2[b,c]	15	75	10
(viii)	11.5	0.165	2[d]	13	49	38
(ix)	5	0.80	2[e]	0	84	16
(x)	5	0.80	2[f]	35	60	5
(xi)	5	0.80	2[c,f]	8	67	25
(xii)	0.5	0.5	2[f]	9	60	31

[a] Reaction under N_2. [b] Initial $[O_2]$; reaction performed in sealed flask. [c] 10% mole ratio of galvinoxyl present. [d] Air bubbled through to ensure O_2 saturation throughout the reaction. [e] Sample stirred rapidly and irradiated. [f] Reaction performed in the dark, with rapid stirring.

as expected for a simple reaction. Good second-order kinetics were observed, and the second-order rate constants at 25 °C were 9.1×10^{-4} M^{-1} s^{-1} and 13×10^{-7} M^{-1} s^{-1} for reaction of **1a** with *n*-PrBr and *i*-PrBr, respectively. This system, with k_2(*n*-PrBr)/k_2(*i*-PrBr) = 700, is more sensitive to steric effects than the more reactive cobaloxime systems for which the ratio of k_2(*n*-PrBr)/k_2(*i*-PrBr) = 14 but is comparable to a rhodium(I) system with k_2(*n*-PrBr)/k_2(*i*-PrBr) = 300.[18,19] The reaction rate was not affected by addition of benzoquinone, by irradiation, or by the presence or absence of oxygen. All of these observations suggest the S_N2 mechanism for this reaction,[2-5,18,19] in contrast with the reactions of *i*-PrI described below.

Reactions with Isopropyl Iodide. A. Characterization and Yields of Products. The reaction of *i*-PrI with **1a** or **1b** in acetone, in the absence of oxygen, gave **3a** or **3b**, respectively. However, in the presence of oxygen, mixtures of the complexes **3**, **4**, and **5** were formed. Complexes **5** could be prepared independently by reaction of iodine with **1**, and analogous products have been observed in other free radical oxidative additions of alkyl iodides.[2-5] However, the (isopropylperoxo)platinum(IV) complexes **4** were not expected and there appear to be no precedents for formation of such alkylperoxo derivatives in oxidative additions of alkyl halides.[8-14] Complexes **4a** and **4b** were characterized by NMR, by elemental analysis, and, for **4a**, by an X-ray structure determination (see later).

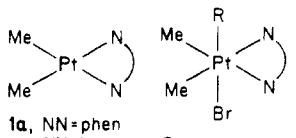

1a, NN = phen
b, NN = bpy

2a, R = *i*-Pr, NN = phen
b, R = *n*-Pr, NN = phen

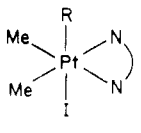

3a, R = *i*-Pr, NN = phen
b, R = *i*-Pr, NN = bpy
c, R = *n*-Pr, NN = phen

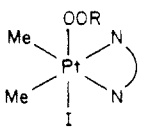

4a, R = *i*-Pr, NN = phen
b, R = *i*-Pr, NN = bpy
c, R = *t*-Bu, NN = phen

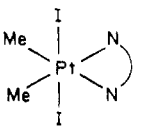

5a, NN = phen
b, NN = bpy

The yields of complexes **3a**, **4a**, and **5a** as a function of reaction conditions wre determined by using ^1H NMR spectroscopy. Typical data are given in Table I. Most of these experiments were conducted in diffuse daylight, and the product yields were different when the experiments were conducted in the dark or when irradiated directly. The results could not be analyzed quantitatively, but the following general trends were noted.

1. The yield of **4a** increased with increasing oxygen concentration, confirming that **4a** is formed from molecular oxygen.

2. Other factors being equal, the yield of **3a** increased and the yield of **5a** decreased with increasing initial concentration of complex **1a**.

3. Other factors being equal, the yield of **3a** was greatest for reactions carried out in the dark and least for reactions carried out with direct irradiation of the solutions.

Scheme I

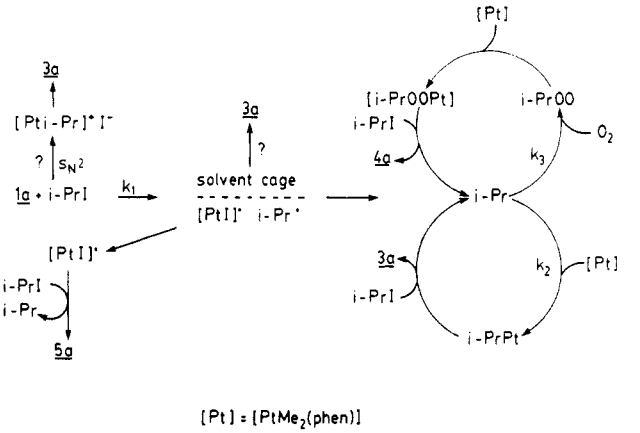

[Pt] = [$PtMe_2$(phen)]

The yields are believed to represent the primary products formed; separate experiments showed that **3a** and **4a** were stable in the presence of *i*-PrI, in the presence or absence of either air or diffuse light, and did not react further to give **5a**. Since complex **5a** is almost certainly formed by the reactions of eq 4 and 5, the yield can give an upper limit on the length of a chain reaction.

$$[PtMe_2(NN)] + i\text{-PrI} \rightarrow [PtIMe_2(NN)]\cdot + i\text{-Pr}\cdot \quad (4)$$

$$[PtIMe_2(NN)]\cdot + i\text{-PrI} \rightarrow [PtI_2Me_2(NN)] + i\text{-Pr}\cdot \quad (5)$$

The extreme range in yields of **5a** was 3–38%, and, since two *i*-Pr radicals are formed for each molecule of **5a**, the maximum length of any radical chain reaction derived from the *i*-Pr· radicals must lie in the range 1.3–17. In the absence of oxygen, a chain length of >1000 has been established.[20] Clearly, oxygen acts as an efficient inhibitor of a chain reaction, and further addition of the radical scavengers galvinoxyl or benzoquinone had little effect on product yields (Table I) or rates (see later).

Much of these data can be rationalized in terms of an inefficient chain reaction as shown in Scheme I.[21] If the reactions of the scheme were efficient, the ratio of products **3a**/**4a** = k_2[**1a**]/$k_3[O_2]$. Thus increasing [**1a**] or decreasing $[O_2]$ should increase the ratio of products **3a**/**4a**. If $k_3 \approx 10^9$ M^{-1} s^{-1} and $k_2 \approx 10^7$ M^{-1} s^{-1} [20-22] and taking a case where $[O_2] \approx$ [**1a**] $\approx 2 \times 10^{-3}$ M, it can be calculated that the product ratio **3a**/**4a** $\approx 10^{-2}$. In practice, more **3a** was almost always formed than predicted by this method, es-

(18) Schrauzer, G. N.; Deutsch, E. *J. Am. Chem. Soc.* **1969**, *91*, 3341.
(19) Collman, J. P.; MacLaury, M. R. *J. Am. Chem. Soc.* **1974**, *96*, 3019.
(20) Hill, R. H.; Puddephatt, R. J. *J. Am. Chem. Soc.* **1985**, *107*, 1218.
(21) Monaghan, P. K.; Puddephatt, R. J. *Organometallics* **1983**, *2*, 1698.
(22) k_3 is approximately the diffusion-controlled rate, and k_2 is estimated from data described previously[20,21] but using a very recently determined rate constant of 5×10^5 M^{-1} s^{-1} for attack of 5-hexenyl radicals on acrylonitrile at room temperature[23] rather than the value of $\sim 2 \times 10^5$ M^{-1} s^{-1} estimated previously.
(23) Giese, B.; Kretzschmar, G. *Chem. Rev.* **1984**, *117*, 3160.

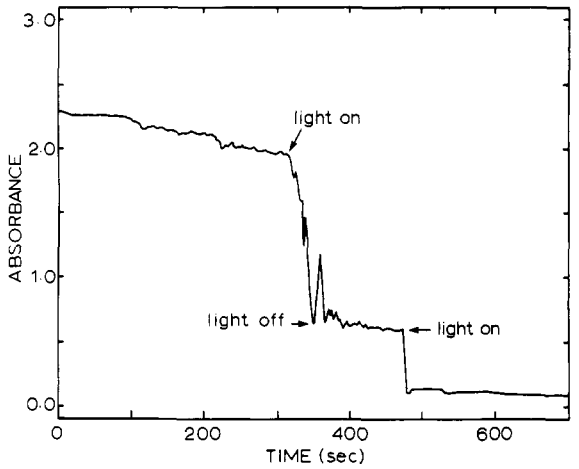

Figure 1. Absorbance vs. time plot for reaction of **1a** with *i*-PrI, showing the effect of light on the rate of reaction. The decay of absorbance due to **1a** at 472 nm was monitored.

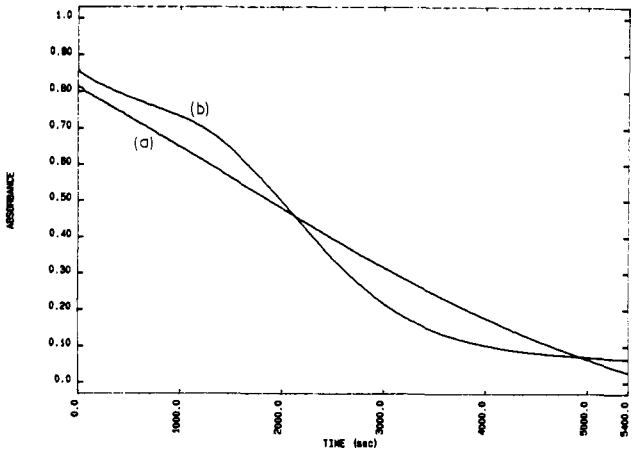

Figure 2. Absorbance (λ = 472 nm.) vs. time plots for reaction of **1a** with *i*-PrI in the dark: (a) in the presence of oxygen; (b) in degassed solution.

pecially from reactions carried out in the dark (Table I). One possible explanation is that the oxygen-centered *i*-PrOO· radical is not trapped efficiently by complex **1a**, but instead often reacts in other ways to terminate the chain.[24] An intriguing possibility to explain the difference in the light and dark reactions is that the dark reaction favors a different mechanism leading only to **3a**. This could involve a radical nonchain process involving recombination within the solvent cage of the radical pair formed in eq 4, or it could involve a competing S_N2 mechanism. In order to explore these possibilities, some kinetic studies were carried out.

B. Kinetic Studies. Rates of disappearance of **1a** were measured by spectrophotometry, monitoring decay of the MLCT band of **1a** centered at 472 nm in acetone solution. Initial studies showed the dramatic effect of light on the rate of reaction (Figure 1). There is no doubt that the light reaction is a free radical chain reaction,[20] and this study is concerned with the dark reaction. In the complete absence of oxygen the dark reaction is also a radical chain process as can be seen by the absorbance vs. time plots of Figure 2. When solutions are degassed rigorously, the reaction was often too fast to monitor but, in other cases in which solutions were degassed only to a residual pressure of 0.1 torr, a short induction period was followed by a rapid loss of **1a**, a typical behavior of radical chain processes. However, in the presence of oxygen or benzoquinone, a much slower reaction was observed. Clearly oxygen acts both as a radical scavenger and a radical chain inhibitor as suggested earlier. Very little oxygen was needed to give this effect; for example, absorbance vs. time plots almost identical with Figure 2b were obtained with solutions from which most of the oxygen had been removed by bubbling nitrogen. A typical set of UV–visible absorption spectra obtained during a kinetic run is shown in Figure 3 (supplementary material).

For reactions in the presence of oxygen, kinetic runs were made over a range of concentrations of *i*-PrI (always in large excess) and complex **1a**. The following features were observed.

1. First-order treatment indicated that the reactions were first order in complex **1a** over the first 40–50% of a given reaction, but then the rate was always faster than predicted towards the end (Figure 4, supplementary material).

2. The initial slopes of first-order plots were independent of the initial concentration of platinum complex **1a**, showing that the reactions are truly first order in **1a** in the initial stages (Figure 4). The rates were not significantly affected by addition of galvinoxyl.

3. The first-order rate constants obtained were directly proportional to the concentration of *i*-PrI, showing a first-order dependence in *i*-PrI. The second-order rate constant was $(3.0 \pm 0.2) \times 10^{-4}$ M^{-1} s^{-1}, covering a range of concentrations of **1a** from 10^{-4} to 10^{-3} M and of *i*-PrI from 0.1 to 0.8 M. The significance of this rate constant is debatable since, even at the very low concentrations of **1a** used in the kinetic runs, there is likely to be some chain reaction occurring. Product analyses (Table I, entry xii) and the failure of radical scavengers to affect the rates suggest that the chain length is unlikely to exceed two under these conditions.

The ratio of true second-order rate constants for the S_N2 reactions of **1a** with *n*-PrI and *n*-PrBr is given by $k_2(n\text{-PrI})/k_2(n\text{-PrBr}) = 3.4 \times 10^{-2}/9.1 \times 10^{-4} = 37$. This is similar to the ratios found for oxidative addition by the S_N2 mechanism of several pairs of alkyl iodides and bromides to cobalamine derivatives.[18] The rate constant for S_N2 oxidative addition of *i*-PrI to **1a** can then be predicted to be $k_2(i\text{-PrI}) \approx 37\ k_2(i\text{-PrBr}) = 4.8 \times 10^{-5}$ M^{-1} s^{-1}. This is approximately 10% of the observed second order rate constants of 3×10^{-4} M^{-1} s^{-1}.

The combined kinetic studies and product analyses lead to the following conclusions.

1. In the light, the reaction of **1a** with *i*-PrI is a free radical chain reaction and is initiated by the photochemical reaction of eq 4. The chain length is, however, low in the presence of oxygen as a result of the isopropylperoxy radicals having a low reactivity for attack on **1a**.

2. In the dark, the reaction largely follows the same path, but it is now initiated by the very slow thermal reaction of eq 4. However, in the presence of oxygen, it is probable that the S_N2 pathway (or possibly a free radical nonchain pathway[25]) is also followed to a minor extent, thus accounting for the relatively higher yields of **3a** in the dark reactions. The observed second-order rate constant for the dark reaction was about 10 times the value pre-

(24) Termination reactions of alkylperoxy radicals have been studied in detail. Kochi, J. K. "Free Radicals"; Wiley: New York, 1973.

(25) This mechanism would require some recombination of the primary radical pair of eq 1 within the solvent cage in the thermal reaction but not in the photochemical reaction. This is not impossible since the radicals would have more kinetic energy and might diffuse apart faster in the photochemical reaction.

(26) Chanon, M. *Bull. Soc. Chim. Fr.* **1982**, *11*, 197.

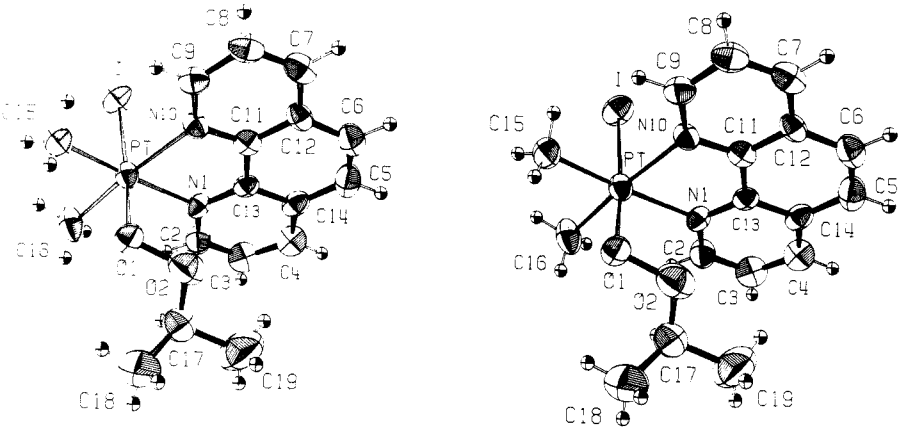

Figure 5. Stereoview of complex **4a** with the crystallographic numbering scheme.

dicted for the S_N2 mechanism, consistent with this hypothesis.

Reaction with *tert*-Butyl Iodide. Reaction of *t*-BuI with **1a** in the absence of air gave only complex **5a**, with the organic products being $Me_2C{=}CH_2$ and Me_3CH as identified by NMR. In the presence of air, the reaction gave a mixture of **5a** and the *t*-BuOOPt derivative **4c**.

Studies of the kinetics of these reactions were difficult because an intermediate having a strong absorbance in the region 350–450 nm was formed. The concentration of this species must be low because it could not be detected by NMR monitoring of reaction mixtures. No CIDNP effects were observed during the reactions. Qualitatively, the reaction of **1a** with *t*-BuI was faster than that with *i*-PrI, and the mechanism is almost certainly a free radical process. In the absence of air the *t*-Bu· radical does not react with **1a**, presumably because of steric hindrance, and hence only **5a** is formed.

Structure of [$PtIMe_2$(OO-*i*-Pr)(1,10-phenanthroline)], 4a. The crystal structure consists of discrete monomeric molecules of iodo(isopropylperoxo)-dimethyl(1,10-phenanthroline)platinum(IV) (Figure 5) with the iodo and isopropylperoxo ligands trans octahedrally coordinated to the *cis*-$PtMe_2$(NN) moiety. The principal coordination dimensions are given in Table II. The Pt–I distance, 2.624 (1) Å, is significantly shorter than most other terminal Pt(IV)–I bonds, for example, in [$PtI_2Me_2(pz_2CH_2)$] [2.651 and 2.647 (1) Å],[27] [$PtI_2C_{10}H_{14}O_4$)] [2.667 (1) Å],[28] Pt(phen)I_6 and Pt(phen)I_5 [range 2.662–2.669 (2) Å],[29] $(C_5H_5NH_2)PtI_6$ [range 2.661–2.670 (1) Å],[30] $(PtI_4)_\infty$ (2.62 Å),[31] and the sum of the covalent radii (2.64 Å);[32] this effect may be attributed to the low trans influence of the alkylperoxo ligand.

The Pt–C distances [2.067 (8) and 2.048 (9) Å] are similar to the corresponding distances in several other methylplatinum(IV) complexes,[27] and the Pt–N distances [2.175 (7) and 2.164 (7) Å] are also in the range of Pt–N distances for platinum(IV) complexes.[27,29,33,34]

Table II. Molecular Dimensions

(a) Bond Distances (Å)			
Pt–I	2.624 (1)	C(5)–C(6)	1.333 (13)
Pt–O(1)	2.032 (6)	C(5)–C(14)	1.436 (13)
Pt–C(15)	2.067 (8)	C(6)–C(12)	1.442 (13)
Pt–C(16)	2.048 (9)	C(7)–C(8)	1.364 (12)
Pt–N(1)	2.175 (7)	C(7)–C(12)	1.396 (13)
Pt–N(10)	2.164 (7)	C(8)–C(9)	1.405 (13)
O(1)–O(2)	1.465 (9)	C(9)–N(10)	1.303 (11)
O(2)–C(17)	1.455 (13)	N(10)–C(11)	1.367 (11)
N(1)–C(2)	1.320 (11)	C(11)–C(12)	1.385 (12)
N(1)–C(13)	1.346 (11)	C(11)–C(13)	1.420 (12)
C(2)–C(3)	1.405 (13)	C(13)–C(14)	1.414 (12)
C(3)–C(4)	1.379 (13)	C(17)–C(18)	1.485 (13)
C(4)–C(14)	1.391 (13)	C(17)–C(19)	1.522 (14)
(b) Bond Angles (deg)			
I–Pt–N(1)	91.2 (2)	C(3)–C(2)–N(1)	122.3 (9)
I–Pt–N(10)	89.1 (2)	C(2)–C(3)–C(4)	118.9 (9)
I–Pt–O(1)	174.6 (2)	C(3)–C(4)–C(14)	119.5 (9)
I–Pt–C(15)	90.6 (3)	C(6)–C(5)–C(14)	121.1 (9)
I–Pt–C(16)	93.0 (3)	C(5)–C(6)–C(12)	121.3 (9)
N(1)–Pt–N(10)	77.0 (3)	C(8)–C(7)–C(12)	119.5 (9)
N(1)–Pt–O(1)	94.2 (2)	C(7)–C(8)–C(9)	117.9 (9)
N(1)–Pt–C(15)	174.7 (3)	C(8)–C(9)–N(10)	124.0 (9)
N(1)–Pt–C(16)	98.4 (3)	C(12)–C(11)–N(10)	121.6 (9)
N(10)–Pt–O(1)	91.5 (3)	C(13)–C(11)–N(10)	117.2 (8)
N(10)–Pt–C(15)	98.0 (3)	C(12)–C(11)–C(13)	121.2 (9)
N(10)–Pt–C(16)	175.0 (3)	C(6)–C(12)–C(7)	122.7 (9)
O(1)–Pt–C(15)	84.1 (3)	C(6)–C(12)–C(11)	118.5 (9)
O(1)–Pt–C(16)	86.8 (3)	C(7)–C(12)–C(11)	118.8 (9)
C(15)–Pt–C(16)	86.5 (4)	C(11)–C(13)–N(1)	119.1 (8)
Pt–O(1)–O(2)	110.2 (4)	C(14)–C(13)–N(1)	121.9 (9)
O(1)–O(2)–C(17)	107.9 (7)	C(11)–C(13)–C(14)	118.9 (9)
Pt–N(1)–C(2)	127.7 (6)	C(4)–C(14)–C(5)	123.2 (9)
Pt–N(1)–C(13)	112.7 (6)	C(4)–C(14)–C(13)	117.9 (9)
C(2)–N(1)–C(13)	119.5 (7)	C(5)–C(14)–C(13)	118.9 (9)
Pt–N(10)–C(9)	128.4 (6)	O(2)–C(17)–C(19)	104.3 (10)
Pt–N(10)–C(11)	113.5 (6)	O(2)–C(17)–C(18)	112.4 (9)
C(9)–N(10)–C(11)	118.2 (8)	C(18)–C(17)–C(19)	110.5 (10)

The Pt(IV)–O distance [2.032 (6) Å] in the title complex is much shorter than those in trimethyl(4,6-dioxonyl)-platinum(IV) dimer (2.15 Å)[35] and in (μ-ethylenediamine)bis[trimethyl(acetylacetonato)platinum(IV)] (2.17 Å)[36] where the very strong trans influence exerted by the methyl groups opposite the Pt–O bonds can be held responsible for long Pt–O distances, whereas trans Pt–O distances of [1.994–1.996 (8) Å] in [$Pt(C_{10}H_{14}O_4)I_2$][28] are slightly shorter than the Pt–O distance in our complex.

The Pt–O(1) line has an angle of 5.3° to the normal of the $PtMe_2$(NN) plane, with O(1) being pushed away from the 1,10-phenanthroline ligand. The isopropylperoxo lig-

(27) Clark, H. C.; Ferguson, G.; Jain, V. K.; Parvez, M., submitted for publication in *Organometallics*.
(28) Cook, P. M.; Dahl, L. F.; Jenkins, R. A. *J. Chem. Soc., Dalton Trans.* **1973**, 294.
(29) Buse, K. D.; Keller, H. J.; Pritzkow, H. *Inorg. Chem.* **1977**, *16*, 1072.
(30) Theile, G.; Wagner, D. *Z. Anorg. Allg. Chem.* **1978**, *446*, 126.
(31) Brodersen, V. K.; Theile, G.; Holle, B. *Z. Anorg. Chem.* **1969**, *369*, 154.
(32) Pauling, L. "The Nature of the Chemical Bond", 3rd ed.; Cornell University Press: Ithaca, NY, 1960.
(33) Brawner, S. A.; Lin, I. J. B.; Kim, J. H.; Everett, G. W. *Inorg. Chem.* **1978**, *17*, 1304.
(34) Larsen, K. P.; Hazell, R. G.; Toftlund, H.; Anderson, P. R.; Bisgard, P.; Edlund, K.; Eliasen, M.; Herskind, C.; Laursen, T.; Pedersen, P. M. *Acta Chem. Scand., Ser. A* **1975**, *A29*, 499.
(35) Swallow, A. G.; Truter, M. R. *Proc. R. Soc. London, Ser. A* **1960**, *A254*, 205.
(36) Robson, A.; Truter, M. R. *J. Chem. Soc.* **1965**, 630.

and is not symmetrically disposed with respect to the phenanthroline ligand (presumably because of packing considerations); thus the N(1)···O(2) and N(10)···O(2) distances are 2.851 and 3.228 Å, respectively, corresponding to torsion angle values N(1)–Pt–O(1)–O(2) = 16.1° and N(10)–Pt–O(1)–O(2) = 61.0°.

The O(1)–O(2) distance [1.465 (9) Å], Pt–O(1)–O(2) and O(1)–O(2)–C(17) angles [110.2 (4)° and 107.9 (7)°, respectively], and the Pt–O(1)–O(2)–C(17) torsion angle (–108.2°) are similar to corresponding values in a [(1-(4-tolyl)ethyl)peroxo]cobalt(III) complex[12] (1.455 Å, 112.8°, 107.2°, and 113.9°, respectively), but there are significant differences from the approximate values reported for *trans*-[PtPh(OO-*t*-Bu)(PPh_3)$_2$][8] [1.22 (3) Å, 116 (1)°, 125 (2)°, and 170.4°, respectively].

Conclusions

The factors influencing the mechanisms of oxidative addition of alkyl halides to transition-metal complexes are becoming clearer.[26] It is particularly important to recognize that steric effects (at either the metal complex or alkyl halide) are greater for the S_N2 mechanism than for the free radical mechanisms. Systems giving the S_N2 mechanism even with secondary alkyl halides are mainly based on square-planar d^8 complexes with ligands which do not block the coordination sites above and below the square plane.[18,19] With d^8 or d^{10} complexes having bulkier ligands the free radical mechanisms are dominant for most alkyl halides.[2-5] Steric effects in complexes 1 are low, and the S_N2 mechanism operates with all primary alkyl halides studied and with isopropyl bromide. However, isopropyl and *tert*-butyl iodides react, at least to a major extent, by a free radical mechanism. It seems that the reaction with isopropyl iodide is close to the borderline where the S_N2 and free radical mechanisms compete and, under conditions where the radical chain mechanism is disfavored, the S_N2 mechanism may become competitive.

Experimental Section

^1H and $^{13}C\{^1H\}$ NMR spectra were recorded by using a Varian XL100 spectrometer, using CD_2Cl_2 or $CDCl_3$ as solvent. UV–visible spectra were recorded by using a Hewlett-Packard 8450A diode array spectrophotometer, and photolysis of the solutions was performed by using a Cole Parmer low noise illuminator, Model 9741-50 (λ range = 400–800 nm). GC was performed by using a Varian Aerograph Series 1400, fitted with a 10% SE-30, 6 ft × $^1/_8$ in. column. Elemental analyses were performed by Guelph Chemical Laboratories. The *i*-PrI and *i*-PrBr used in this work were purified by distillation using a spinning band fractionating column. *t*-BuI was washed with saturated aqueous $Na_2S_2O_3$ solution to remove I_2, then separated, dried with $MgSO_4$, and distilled under vacuum. Complexes **1a** and **1b** were prepared as described previously.[21] The hydrogen atoms of the phenanthroline ligands are defined as previously;[6,21] thus H^2 is adjacent to nitrogen and H^3, H^4, and H^5 then follow around the ring.

[PtIMe$_2$(*i*-Pr)(phen)]. To a solution of [$PtMe_2$(phen)] (0.078 g) in dry, deoxygenated acetone (50 mL) was added *i*-PrI (3 mL). The solution color changed from orange to pale yellow as reaction proceeded. After 40 min, the volume was reduced and pentane (20 mL) was added to precipitate the product: yield 84%; mp 196 °C. Anal. Calcd for $C_{17}H_{21}IN_2Pt$: C, 35.5; H, 3.7; N, 4.9. Found: C, 35.3; H, 3.5; N, 5.9. NMR (CD_2Cl_2): δ_H 1.58 [s, ^2J(PtH) = 72 Hz, MePt], 0.16 [d, ^3J(HH) = 6.5 Hz, ^3J(PtH) = 63 Hz, MeC], 1.81 [septet, ^3J(HH) = 6.5 Hz, Me_2CH], 9.32 [m, $J(H^2H^3)$ = 5 Hz, $J(H^2H^4)$ = 1 Hz, J(PtH) = 15 Hz, H_2], 8.00 [m, $J(H^3H^4)$ = 8.1 Hz, H_3], 8.64 [m, H^4], 8.08 [s, H^5]; δ_C –3.48 [q, ^1J(PtC)730, MePt], 24.47 [q, ^2J(PtC)32, *Me*C], 28.12 [d, Me_2CH].

Similarly the following were prepared. [PtIMe$_2$(*i*-Pr)(bpy)]: yield 85%. NMR (CD_2Cl_2): δ_H 1.40 [s, ^2J(PtH) = 72 Hz, MePt], 0.19 [d, ^3J(HH) = 7 Hz, ^3J(PtH) = 61 Hz, MeC], 1.73 [septet, $CHMe_2$]. [PtBrMe$_2$(*i*-Pr)(phen)]: yield 85%; mp 230 °C dec. Anal. Calcd for $C_{17}H_{21}BrN_2Pt$: C, 38.6; H, 4.0; N, 5.2. Found: C, 38.7; H, 4.1; N, 5.3. NMR (CD_2Cl_2): δ_H 1.51 [s, ^2J(PtH) = 72 Hz, MePt], 0.19 [d, ^3J(HH) = 7 Hz, ^3J(PtH) = 64 Hz, MeC], 9.21 [m, H^2], 7.89 [m, H^3], 8.48 [7, H^4], 7.95 [s, H^5], Me_2CH resonance obscured. [PtBrMe$_2$(*n*-Pr)(phen)]: yield 82%; mp 268 °C dec; NMR (CD_2Cl_2) δ_H 1.47 [s, ^2J(PtH) = 71 Hz, MePt], 0.50 [t, ^3J(HH) = 7 Hz, CH_3C], 9.22 [m, $J(H^2H^3)$ = 5 Hz, $J(H^2H^4)$ = 1.5 Hz, H^2], 7.96 [m, $J(H^3H^4)$ = 8 Hz, H^3], 8.58 [m, H^4], 8.04 [s, H^5].

[PtIMe$_2$(OO-*i*-Pr)(phen)]. Excess *i*-PrI (2.0 mL) was added to a rapidly stirred solution of [$PtMe_2$(phen)] (0.05 g) in acetone (25 mL) in a flask which was open to the atmosphere. The solution changed color from orange to yellow. After 1 h, the volume was reduced to 3 mL and pentane (20 mL) was added to precipitate the product. This was purified by chromatography on a silica gel column, eluting first with CH_2Cl_2/acetone (10:1) to give the impurity of complex **5a** and then with acetone to give the product; yield 54%. Anal. Calcd for $C_{17}H_{21}IN_2O_2Pt$: C, 33.6; H, 3.5; N, 4.6; O, 5.3. Found: C, 34.2; H, 3.3; N, 4.6; O, 5.3. NMR (CD_2Cl_2): δ_H 2.03 [s, ^2J(PtH) = 72 Hz, MePt], 0.31 [d, ^3J(HH) = 6 Hz, MeC], 3.10 [septet, Me_2CH], 9.40 [m, $J(H^2H^3)$ = 5 Hz, $J(H^2H^4)$ = 1.2 Hz, J(PtH) = 18 Hz, H_2], 8.03 [m, $J(H^3H^4)$ = 8 Hz, H_3], 8.60 [m, H^4], 8.08 [s, H^5]; δ_C –4.61 [^1J(PtC) = 600 Hz, MePt], 19.88 [CH_3C], 75.39 [^3J(PtC) = 150 Hz, Me_2CH].

Similarly was prepared [PtIMe$_2$(OO-*i*-Pr)(bpy)]. NMR (CD_2Cl_2): δ_H 1.83 [s, ^2J(PtH) = 72 Hz, MePt], 0.51 [d, ^3J(HH) = 6 Hz, MeC], 3.22 [septet, Me_2CH], 8.97 [m, $J(H^5H^6)$ = 5 Hz, $J(H^4H^6)$ = 1.5 Hz, H^6], 7.65 [m, $J(H^4H^5)$ = 7 Hz, H^5], 8.04 [m, H^4], 8.24 [m, H^3].

[PtIMe$_2$(OO-*t*-Bu)(phen)]. To a rapidly stirred solution of [$PtMe_2$(phen)] (0.07 g) in CH_2Cl_2 (20 mL), in a flask open to the atmosphere, was added freshly purified *t*-BuI (0.2 mL). The solution color changed from orange to yellow over a period of 1 h. The solvent volume was reduced, and the product, contaminated with [PtI_2Me_2(phen)], was precipitated with pentane. It is important to isolate the product at this stage; solutions left for longer periods in contact with excess *t*-BuI became brown in color, and only [PtI_2Me_2(phen)] could be isolated. The product was purified by column chromatography as described above; yield 60%. Anal. Calcd for $C_{18}H_{23}IN_2O_2Pt$: C, 34.8; H, 3.7; N, 4.5. Found: C, 34.7; H, 3.6; N, 4.4. NMR (CD_2Cl_2): δ_H 1.92 [s, ^2J(PtH) = 72 Hz, MePt], 0.26 [s, CH_3C], 9.32 [m, $J(H^2H^3)$ = 5 Hz, $J(H^2H^4)$ = 1.5 Hz, H^2], 8.00 [m, $J(H^3H^4)$ = 8 Hz, H^3], 8.58 [m, H^4], 8.05 [s, H^5]; δ_C –4.17 [^1J(PtC) = 630 Hz, MePt], 26.04 [CH_3C], 76.40 [CO].

Product Analyses. Reactions of **1a** with *i*-PrI in acetone were carried out under various conditions (Table I). When reaction was complete, solvents were removed under vacuum and the crude products were dissolved in $CDCl_3$. Yields (Table I) were then determined by integration of the NMR spectra.

Reactions of **1a** in acetone with mixtures of a large excess of *i*-PrBr and different amounts of *n*-PrBr (concentration of *n*-PrBr = 0–2 × 10^{-2}[*i*-PrBr]) were carried out similarly, and analysis of the ratio of products **2a**/**2b** was again carried out by NMR.

Kinetic Studies. In a typical experiment a solution of [$PtMe_2$(phen)] in acetone (5 mL, 3 × 10^{-4} M) was placed in a quartz cuvette (1 cm) in the cell compartment of the spectrophotometer. The required amount of *i*-PrI was added, the solution was stirred, and then the decay of the absorbance at 472 nm was monitored with time. In other experiments complete UV–visible spectra were recorded (300–600 nm) as a function of time. When the effect of light on the rate was studied, the solutions were made up as above but the solution was irradiated periodically from above. To partially deoxygenate solutions when required, the acetone solution in a cuvette fitted with a serum cap was purged with pure dry nitrogen prior to addition of *i*-PrI. For rigorously deoxygenated solutions, the acetone solution was subjected to five freeze–pump–thaw cycles in an all glass apparatus with two side arms fitted with a cuvette and a tube containing the required amount of *i*-PrI. The *i*-PrI and the acetone solution were mixed, and the mixture was poured into the cuvette for monitoring by UV–visible spectroscopy as above.

X-ray Structure Analysis. Crystals of [PtIMe$_2$(OO-*i*-Pr)(phen)] (**4a**) were grown by slow diffusion of ether into a CH_2Cl_2 solution at –5 °C.

Crystal data for **4a**: $C_{17}H_{21}IN_2O_2Pt$, M_r = 607.4, monoclinic, a = 9.946 (2) Å, b = 11.340 (3) Å, c = 16.374 (2) Å, β = 94.55 (1)°, U = 1841.0 Å^3, Z = 4, D_{calcd} = 2.19 g cm^{-3}, F(000) = 1136, Mo Kα radiation, λ = 0.710 69 Å, μ(Mo Kα) = 97.2 cm^{-1}; space group

$P2_1/n$ from systematic absences $h0l$ if $h + l = 2n + 1$ and $0k0$ if $k = 2n + 1$.

Data were collected to a maximum θ of 20° on an Enraf-Nonius CAD4 diffractometer by the $\omega/2\theta$ scan method using monochromatized Mo Kα radiation, with a crystal of dimensions 0.088 × 0.100 × 0.125 mm, bound by faces 101, $\bar{1}0\bar{1}$, $10\bar{1}$, $\bar{1}01$, $11\bar{1}$, $\bar{1}\bar{1}1$, $1\bar{1}\bar{1}$, and $\bar{1}11$. Following machine location and centering of 25 reflections with θ in the range $10 < \theta < 15°$, accurate cell constants and the orientation matrix were obtained by a least-squares refinement. A total of 1710 reflections were collected of which 1402 had intensities greater than $3\sigma(I)$ and were used in structure solution and refinement. Data were corrected for Lorentz and polarization factors and for absorption. Maximum and minimum values of the transmission coefficients are 0.5553 and 0.3824, respectively.

The coordinates of the Pt and I atoms were obtained from an analysis of a three-dimensional Patterson function and the remaining non-hydrogen atoms were located from a heavy-atom-phased Fourier map.[37] Initial refinement by full-matrix least-squares calculations with isotropic temperature factors for non-hydrogen atoms lowered R to 0.074 which further dropped to 0.044 after six cycles of anisotropic refinement. A difference map computed at this stage revealed maxima (0.7–0.4 e/Å^3) corresponding to the 21 hydrogen atoms which were included in the subsequent refinement in geometrically idealized positions (C–H = 0.95 Å); an overall isotropic thermal parameter was allowed to refine for the hydrogen atoms. In the final six rounds of least-squares cycles, a weighting scheme of the form $w^{1/2} = [\sigma^2 F + pF^2]^{-1/2}$ was employed where the final p parameter was 0.00015. Scattering factors used in the structure factor calculations were taken from ref 38 for non-hydrogen atoms and ref 39 for hydrogen atoms, and allowance was made for anomalous dispersion.[40] Refinement converged with $R = 0.0230$ and $R_w = [\sum w\Delta^2/\sum wF_o^2]^{1/2} = 0.0245$ for the 1402 reflections with $I > 3\sigma(I)$. The maximum shift/error ratios were −0.008 for the x coordinate of C(19) and −0.011 for U_{22} of C(6). A final difference map was devoid of any significant features. Final fractional coordinates with estimated standard deviations are in Table III. The structure factor listing (Table IV), calculated hydrogen coordinates (Table V), thermal parameters (Table VI), and mean plane data (Table VII) have been deposited as supplementary material.

Acknowledgment. We thank NSERC (Canada) for financial support.

Registry No. **1a**, 52594-55-5; **1b**, 52594-52-2; **2a**, 97523-02-9; **2b**, 97523-03-0; **3a**, 87318-07-8; **3b**, 97523-04-1; **4a**, 87318-06-7; **4b**, 97523-05-2; **4c**, 97523-06-3; **5a**, 86407-72-9; **5b**, 85027-40-3; *i*-PrI, 75-30-9; *t*-BuI, 558-17-8; *i*-PrBr, 75-26-3; *n*-PrBr, 106-94-5; O_2, 7782-44-7.

Supplementary Material Available: Figure 3, changes in absorption spectra during reaction of **1a** with *i*-PrI, Figure 4, first-order kinetic plots for reaction of **1a** with *i*-PrI in the dark, Table IV, observed and calculated structure amplitudes, Table V, calculated hydrogen coordinates, Table VI, thermal parameters, and Table VII, mean plane data (11 pages). Ordering information is given on any current masthead page.

(37) Sheldrick, G. M. SHELX '76, A program system for crystal structure determination, University of Cambridge, England.

(38) Cromer, D. T.; Mann, J. B. *Acta Crystallogr., Sect. A: Cryst. Phys., Diffr., Theor. Gen. Crystallogr.* **1968**, *A24*, 321.

(39) Stewart, R. F.; Davidson, E. R.; Simpson, W. T. *J. Chem. Phys.* **1965**, *42*, 3175.

(40) Cromer, D. T.; Liberman, D. *J. Chem. Phys.* **1970**, *53*, 1891.